AMERICAN SOCIETY FOR MICROBIOLOGY | Journal of Virology®

VIRUS-CELL INTERACTIONS

HIF1α-Regulated Expression of the Fatty Acid Binding Protein Family Is Important for Hypoxic Reactivation of Kaposi's Sarcoma-Associated Herpesvirus

Rajnish Kumar Singh,[a]* Dipayan Bose,[a] Erle S. Robertson[a,b]

[a]Department of Otorhinolaryngology-Head and Neck Surgery, Perelman School of Medicine, University of Pennsylvania, Philadelphia, Pennsylvania, USA
[b]The Tumor Virology Program, Abramson Cancer Center, Perelman School of Medicine, University of Pennsylvania, Philadelphia, Pennsylvania, USA

ABSTRACT The hypoxic microenvironment and metabolic reprogramming are two major contributors to the phenotype of oncogenic virus-infected cells. Infection by Kaposi's sarcoma-associated herpesvirus (KSHV) stabilizes hypoxia-inducible factor 1α (HIF1α) and reprograms cellular metabolism. We investigated the comparative transcriptional regulation of all major genes involved in fatty acid and amino acid metabolism in KSHV-positive and -negative cells grown under normoxic or hypoxic conditions. We show a distinct regulation of genes involved in both fatty acid and amino acid metabolism in KSHV-positive cells grown in either normoxic or hypoxic conditions, with a particular focus on genes involved in the acetyl coenzyme A (acetyl-CoA) pathway. The fatty acid binding protein (FABP) family of genes, specifically FABP1, FABP4, and FABP7, was also observed to be synergistically upregulated in hypoxia by KSHV. This pattern of FABP gene expression was also seen in naturally infected KSHV BC3 or BCBL1 cells when compared to KSHV-negative DG75 or BL41 cells. Two KSHV-encoded antigens, which positively regulate HIF1α, the viral G-protein coupled receptor (vGPCR), and the latency-associated nuclear antigen (LANA) were shown to drive upregulation of the FABP gene transcripts. Suppression of FABPs by RNA interference resulted in an adverse effect on hypoxia-dependent viral reactivation. Overall, this study provides new evidence, which supports a rationale for the inhibition of FABPs in KSHV-positive cells as potential strategies, for the development of therapeutic approaches targeting KSHV-associated malignancies.

IMPORTANCE Hypoxia is a detrimental stress to eukaryotes and inhibits several cellular processes, such as DNA replication, transcription, translation, and metabolism. Interestingly, the genome of Kaposi's sarcoma-associated herpesvirus (KSHV) is known to undergo productive replication in hypoxia. We investigated the comparative transcriptional regulation of all major genes involved in fatty acid and amino acid metabolism in KSHV-positive and -negative cells grown under normoxic or hypoxic conditions. Several metabolic pathways were observed differentially regulated by KSHV in hypoxia, specifically, the fatty acid binding protein (FABP) family genes (FABP1, FABP4, and FABP7). KSHV-encoded antigens, vGPCR and LANA, were shown to drive upregulation of the FABP transcripts. Suppression of FABPs by RNA interference resulted in an adverse effect on hypoxia-dependent viral reactivation. Overall, this study provides new evidence, which supports a rationale for the inhibition of FABPs in KSHV-positive cells as potential strategies, for the development of therapeutic approaches targeting KSHV-associated malignancies.

KEYWORDS fatty acid binding proteins, hypoxia, KSHV, LANA, reactivation, vGPCR

Kaposi's sarcoma-associated herpesvirus (KSHV) is a large double-stranded DNA (dsDNA) virus of approximately 170 kb in size and is an oncogenic gamma

Citation Singh RK, Bose D, Robertson ES. 2021. HIF1α-regulated expression of the fatty acid binding protein family is important for hypoxic reactivation of Kaposi's sarcoma-associated herpesvirus. J Virol 95:e02063-20. https://doi.org/10.1128/JVI.02063-20.

Editor Jae U. Jung, Lerner Research Institute, Cleveland Clinic

Address correspondence to Erle S. Robertson, erle@pennmedicine.upenn.edu.

* Present address: Rajnish Kumar Singh, Molecular Biology Unit, Institute of Medical Sciences, Banaras Hindu University, Varanasi, UP, India.

Received 22 October 2020
Accepted 28 March 2021
Accepted manuscript posted online 31 March 2021
Published 24 May 2021

herpesvirus, which is a major challenge in immunocompromised malignancies (1, 2). Kaposi's sarcoma (KS), primary effusion lymphoma (PEL), multicentric Castleman disease (MCD), and KSHV inflammatory cytokine syndrome (KICS) are the major diseases associated with KSHV infection (3). This virus shows a typical pattern of its life cycle, similar to other oncogenic *Herpesviridae*, where it can establish either a latent phase or a lytic cycle in infected cells (4). During the latent phase of infection, a selected set of genes with high oncogenic potential are expressed (5). The major latency protein, latency-associated nuclear antigen (LANA), is responsible for tethering KSHV episomes to the host genome and interacts with other cellular proteins to promote the oncogenic characteristics of infected cells (6–8). Other KSHV antigens that are expressed in the majority of KSHV-associated tumor biopsy samples are vFLIP, vCyclin, K1, K2, all KSHV-encoded microRNA, and the vIRF3 (LANA2) (6, 9). In addition, certain KSHV-associated biopsy samples have also been shown to express both viral G-protein coupled receptor (vGPCR) and K1 (10). The major complement of latent or lytic antigens encoded by KSHV was predicted and has the potential for modulating several signaling pathways, ultimately leading to promotion of a precancerous phenotype (11–14). The latency to lytic shift of KSHV is also known to be a result of epigenetic changes within the KSHV genome, where hypoxia alone or in combination with chemical epigenetic modifiers such as 12-*O*-tetradecanoylphorbol-13-acetate (TPA) and butyric acid (BA) can actively promote lytic reactivation (15–18). KSHV-encoded LANA can interact directly with hypoxia-inducible factor 1α (HIF1α), a crucial effector of hypoxia to promote reactivation, and can modulate expression of the replication and transcriptional activator (RTA). This demonstrates an essential role during both latent and lytic replication of KSHV (19). Interestingly, LANA creates a positive feedback loop to maintain high HIF1α levels by degrading VHL protein (20), which is a well-known tumor suppressor and negative regulator of HIF1α (20–22). Moreover, HIF1α has been shown to upregulate transcription of LANA by transactivating hypoxia responsible elements (HREs) within the LANA promoter (constitutive latent transcription promoter, LTc) (23). Interestingly, RTA can also activate transcription of the major latency locus to maintain enhanced levels of LANA (24).

Hypoxia, a potent inhibitor of DNA replication in eukaryotes (25–27), was previously shown to paradoxically mediate KSHV reactivation (28, 29). We recently observed that KSHV-encoded LANA protects several replication-associated proteins from hypoxia-mediated degradation and, hence, plays a crucial role in hypoxic reactivation of KSHV (30). However, the required cellular metabolic reprogramming in KSHV-positive cells in hypoxic conditions is still not well-understood (31). Using whole transcriptomics, we recently observed global metabolic reprogramming in KSHV-infected B-cells grown under hypoxic conditions (31). The study showed that KSHV-encoded vGPCR was transcriptionally regulated by the host hypoxia-inducible transcription factor, HIF1α. KSHV-encoded vGPCR in turn is known to upregulate expression of HIF1α by acting through the P38-mitogen-activated protein kinase (MAPK) pathway (32). This explains another feedback mechanism of upregulated expression of HIF1α in KSHV-infected cells. Though, the study has provided several new insights regarding the mechanisms and pathways linked to transcription reprogramming, like other high-throughput experiment-based studies, a large variability in the expression of several genes was observed. This led to the observation of a difference of expression for many candidate genes, which were not significant, but necessitated a more stringent study on large sets of genes involved in metabolic pathways in KSHV-positive cells grown in hypoxic conditions. In this present study, we used real-time PCR-based screening to identify differential expression of metabolic genes, with a focus on those genes that belong to fatty acid and protein metabolism pathways. Categorically, these genes are members of the acetyl coenzyme A (acetyl-CoA), triacylglycerol, fatty acid transport, carnitine, ketogenesis, and ketone body, as well as genes of the amino acid metabolic pathways.

The results of the study demonstrated a dominant role of hypoxia in downregulation of expression of several genes involved in fatty acid and amino acid metabolism in

both KSHV-negative BJAB, and KSHV-positive BJAB-KSHV cells. However, a number of genes showed a profile that was opposite in expression in that it showed upregulated expression. Nevertheless, a comparative study between BJAB and BJAB-KSHV cells showed a pattern of expression where we observed upregulation, downregulation, as well as little or no detectable change in expression pattern of some genes. Furthermore, the study also identified genes that are members of the fatty acid binding protein (FABP) family of proteins, which were upregulated during hypoxic conditions in both BJAB and BJAB-KSHV cells. Normoxic BJAB-KSHV cells also showed a high endogenous level for FABPs, particularly for FABP1, FABP4, and FABP7. Moreover, upregulated FABP expression was synergistic in terms of expression in BJAB-KSHV cells grown under hypoxic conditions compared to that of normoxic BJAB-KSHV or hypoxic BJAB cells.

Fatty acid binding proteins are a family of low-molecular-weight proteins (14 to 15 kDa), with a vast role in metabolic diseases (33). These proteins work as chaperones for long-chain fatty acids and related hydrophobic molecules to facilitate their transportation in aqueous medium (34). FABPs have also been reported to have implications in brain development and diseases, cardiovascular and metabolic diseases, celiac disease enteropathy, and other diseases (33, 35–37). Expression of different FABPs is tissue specific and is controlled at the transcript level (34, 38–40). In general, FABPs are named based on the organ system from which they were originally isolated, such as A-FABP (adipocyte), H-FABP (heart), B-FABP (brain), E-FABP (epidermis or psoriasis-associated), L-FABP (liver), I-FABP (intestine), and P2-FABP (myelin or P2) (40). This nomenclature does not always follow the same pattern of expression in a specific organ, as L-FABP was later proposed as a novel marker for kidney disease (41). Identification of elevated expression of FABP1 (L-FABP), FABP4 (A-FABP), and FABP7 (B-FABP) in KSHV-positive cells in hypoxia prompted us to investigate the role of these FABPs in KSHV biology in detail. We showed that hypoxia-induced KSHV-encoded antigens LANA and vGPCR have the potential for positive feedback to upregulate HIF1α levels, leading to upregulated expression of FABPs. Our investigations led us to identify a role for FABPs in KSHV biology and showed a compromised potential for reactivation under hypoxic conditions. Altogether, this study provides an additional strategy to target FABPs for development of novel therapeutic approaches to target KSHV-associated diseases.

RESULTS

Transcriptional regulation of fatty acid metabolism-associated genes by KSHV in hypoxia. To study the role of KSHV infection in transcriptional regulation of genes involved in fatty acid metabolism, KSHV-negative and KSHV-positive BJAB cells with an isogenic background and similar passage numbers were selected. Characterizations of these cell lines were described earlier (31). Hypoxia was induced and confirmation of hypoxic induction was confirmed by analyzing expression of a hypoxia-inducible factor 1α (HIF1α) transcriptional target, P4HA1 (Fig. 1A). A list of genes involved in fatty acid metabolism was identified, and real-time PCR primers were designed (see Table S1 in the supplemental material). The differential expression of fatty acid metabolism-associated genes was studied by quantitative real-time PCR. In brief, the fatty acid metabolic pathways investigated included acetyl-CoA metabolism, carnitine transferase, fatty acid transport, ketogenesis and ketone body metabolism, and triacylglycerol metabolism. The analysis of real-time PCR assays showed that induction of hypoxia had a dominating potential with few exceptions. Most of the genes were downregulated in both BJAB and BJAB-KSHV cells in hypoxia (Fig. 1B to F). The downregulated genes were distributed throughout the different pathways involved in fatty acid metabolism mentioned above. However, several transcripts were also seen downregulated in the KSHV-positive background without hypoxia induction. Furthermore, we also observed upregulated genes in both BJAB and BJAB-KSHV cells grown in hypoxia, such as ACADL, ACADVL, ACSBG1, ACSL3, ACOT6, ACOT12, PRKAA2, PRKAB1, and PRKACA (all from the acetyl-CoA metabolic pathway) (Fig. 1B); FABP1, FABP3, FABP4, and FABP7 (from the fatty acid transport pathway) (Fig. 1C); and CPT1C and CROT (the carnitine

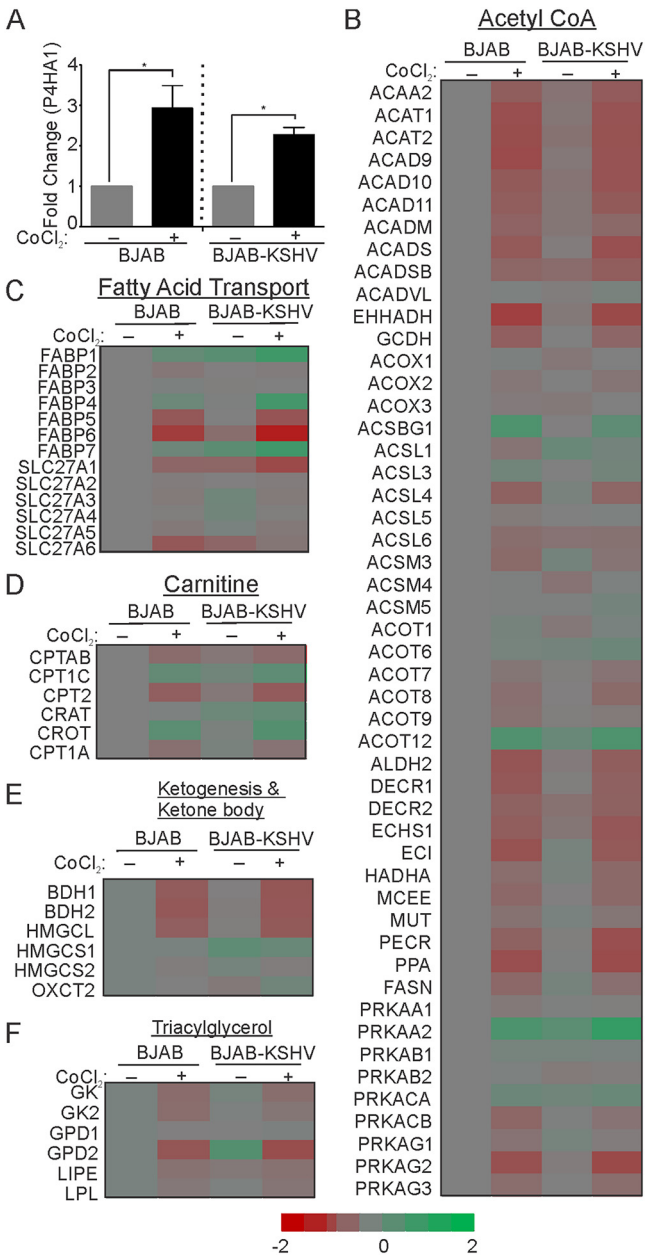

FIG 1 Transcriptional status of genes involved in fatty acid metabolism in BJAB and BJAB-KSHV cells grown under normoxic or hypoxic conditions. Cells were grown for 48 h in normoxic or $CoCl_2$-induced hypoxic conditions. Equal amounts of cDNA were used to perform real-time PCR, taking GAPDH as an endogenous control. All fold change expression is represented in the scale of $\log_{10}$. (A) Confirmation of hypoxia induction in BJAB and BJAB-KSHV cells. BJAB and BJAB-KSHV cells were grown in medium with or without $CoCl_2$ for 48 h. RNA was extracted using the standard phenol-chloroform extraction method, and 2 μg of RNA was used for cDNA synthesis according to manufacturer protocol. One microliter of 10-times diluted cDNA was used for quantitative analysis of HIF1α transcriptional target P4HA1 using GAPDH as an endogenous control. (B) Fold change expression of genes involved in acetyl-CoA metabolism in normoxic BJAB-KSHV or hypoxic BJAB and BJAB-KSHV cells compared to that in normoxic BJAB cells. (C) Fold change expression of genes involved in fatty acid transport in normoxic BJAB-KSHV or hypoxic BJAB and BJAB-KSHV cells compared to that in normoxic BJAB cells. (D) Fold change expression of genes involved in carnitine metabolism in normoxic BJAB-KSHV or hypoxic BJAB and BJAB-KSHV cells compared to that in normoxic BJAB cells. (E) Fold change expression of genes involved in ketogenesis and ketone body metabolism in normoxic BJAB-KSHV or hypoxic BJAB and BJAB-KSHV cells compared to that in normoxic BJAB cells. (F) Fold change expression of genes involved in triacylglycerol metabolism in normoxic BJAB-KSHV or hypoxic BJAB and BJAB-KSHV cells compared to that in normoxic BJAB cells.

pathway) (Fig. 1D). Most of the studied transcripts from ketogenesis and ketone body and triacylglycerol metabolic pathways were downregulated in BJAB-KSHV cells under hypoxia compared to those of control BJAB cells (Fig. 1E and F). Moreover, we also identified distinct transcripts, which were upregulated under a KSHV-positive background and were independent of hypoxia induction. For example, we observed ACADL, ACSL1, ACSL4, ACSM3, ACOT6, ECI, HADHA, MUT, FASN, PRKAA2, PRKACA, and PRKAGA1 (acetyl Co-A pathway); FABP1, FABP4, FABP7, SLC27A3, SLC27A4, and SLC27A5 (fatty acid transport genes); CPT1C, CRAT, CROT, and CPT1A (carnitine pathway genes); HMGCS1 and HMGCS2 (ketogenesis and ketone body pathway); and GK and GPD2 (triacylglycerol pathway) were specifically upregulated in BJAB- KSHV cells. These results suggested that a certain antigen(s) encoded by KSHV can transactivate expression of these genes.

Transcription regulation of amino acid metabolism-associated genes by KSHV in hypoxia. We extended our study of differential gene expression of BJAB or BJAB-KSHV cells in hypoxia as well as normoxia for the genes involved in amino acid metabolism. Briefly, we selected genes from the arginine, glutamine, glutamate, leucine, proline, tryptophan, methionine, isoleucine, histidine, alanine, phenylalanine, serine, glycine, threonine, tyrosine, and valine metabolic pathways. A list of real-time PCR primers used to study differential expression of genes involved in amino acid metabolism is provided in Table S1. Similar to fatty acid metabolic pathway genes, we showed that hypoxia also had a dominant role in downregulating expression of genes that are involved in amino acid metabolism (Fig. 2A to M). We showed that genes involved in arginine metabolism, except for AOC1, AMD1, and SAT1, were downregulated in hypoxia (Fig. 2A). Interestingly, we also observed that AGMAT was upregulated in KSHV-positive BJAB cells, and its expression further showed a synergistic upregulation in hypoxia. However, expression of AGMAT was negatively regulated in BJAB cells grown in hypoxia (Fig. 2A). Among the genes from the glutamine and glutamate pathway, NIT2 and PPAT were shown to be upregulated in KSHV-positive BJAB cells where PPAT showed a synergistic upregulation under hypoxic condition. Furthermore, GLS was observed to be slightly upregulated only in BJAB-KSHV cells grown in hypoxia (Fig. 2M). Among the proline, leucine, isoleucine, and tyrosine metabolic pathways, almost all genes showed downregulation in hypoxic conditions, except for AOX1 (leucine metabolic pathway), PRODH2 (proline metabolic pathway), HGD, and TPO (tyrosine metabolic pathway). Interestingly, most of the genes from these pathways were also found to be marginally or moderately downregulated in BJAB-KSHV cells grown in normoxia compared to those in BJAB cells, except for BCAT1 and IARS of the isoleucine metabolic pathway and DBH, HGD, and PNMT of the tyrosine metabolic pathway (Fig. 2K, C, F, and E). Similarly, hypoxia showed a dominant effect on expression of genes in the methionine, phenylalanine, valine, serine, glycine, and threonine biosynthetic pathways, where most genes showed downregulated expression in BJAB or BJAB-KSHV cells grown in hypoxia compared to that in BJAB cells. The only exceptions were MAT1A (the methionine metabolic pathway), and HPD and PAH (the phenylalanine metabolic pathway), where MAT1A was observed to be upregulated in both BJAB and BJAB-KSHV cells grown in hypoxia and HPD and PAH were upregulated in only BJAB-KSHV cells grown in hypoxia. Interestingly, most of the genes involved in these pathways were downregulated in both BJAB-KSHV and BJAB cells grown in normoxia (Fig. 2D, I, H, and L). In the lysine metabolic pathway, most of the genes were downregulated in BJAB grown in hypoxia as well as BJAB-KSHV cells grown in normoxia. Interestingly, BJAB-KSHV grown in hypoxia showed a small activating effect that elevated the expression of the lysine metabolic pathway genes (Fig. 2G).

The tryptophan and histidine metabolic pathway-associated genes showed a comparatively different response compared to that of other amino acid metabolic pathway genes (Fig. 2B and J). Here, we observed that hypoxia did not have a dominant suppressive role in the expression of genes involved in these pathways, especially in KSHV-negative BJAB cells. Genes AADAT, ACMSD, DDC, KMO and TPH2 (tryptophan metabolic pathway), FTCD, HDC, HNMT, and MAOA (histidine metabolic pathway) were

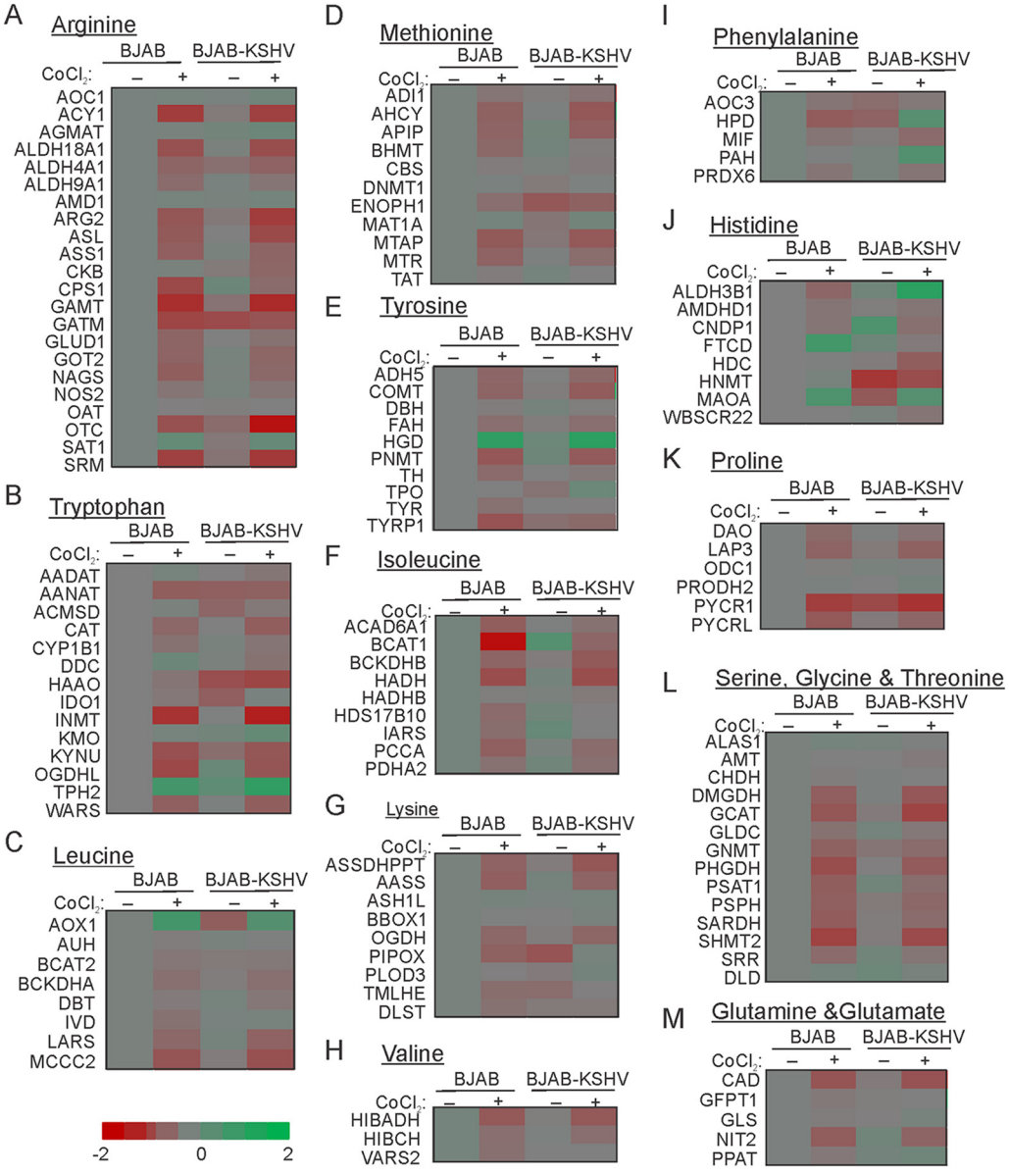

FIG 2 Transcriptional status of genes involved in amino acid metabolism in BJAB and BJAB-KSHV cells grown under normoxic or hypoxic conditions. Cells were grown for 48 h in normoxic or $CoCl_2$-induced conditions followed by calculating fold change expression of target genes using GAPDH as an endogenous control. All fold change expression is represented in the scale of log_{10}. (A) Fold change expression of genes involved in arginine metabolism in normoxic BJAB-KSHV or hypoxic BJAB and BJAB-KSHV cells compared to that in normoxic BJAB cells. (B) Fold change expression of genes involved in tryptophan in normoxic BJAB-KSHV or hypoxic BJAB and BJAB-KSHV cells compared to that in normoxic BJAB cells. (C) Fold change expression of genes involved in leucine metabolism in normoxic BJAB-KSHV or hypoxic BJAB and BJAB-KSHV cells compared to that in normoxic BJAB cells. (D) Fold change expression of genes involved in methionine metabolism in normoxic BJAB-KSHV or hypoxic BJAB and BJAB-KSHV cells compared to that in normoxic BJAB cells. (E) Fold change expression of genes involved in tyrosine metabolism in normoxic BJAB-KSHV or hypoxic BJAB and BJAB-KSHV cells compared to that in normoxic BJAB cells. (F) Fold change expression of genes involved in isoleucine metabolism in normoxic BJAB-KSHV or hypoxic BJAB and BJAB-KSHV cells compared to that in normoxic BJAB cells. (G) Fold change expression of genes involved in lysine metabolism in normoxic BJAB-KSHV or hypoxic BJAB and BJAB-KSHV cells compared to that in normoxic BJAB cells. (H) Fold change expression of genes involved in valine metabolism in normoxic BJAB-KSHV or hypoxic BJAB and BJAB-KSHV cells compared to that in normoxic BJAB cells. (I) Fold change expression of genes involved in phenylalanine metabolism in normoxic BJAB-KSHV or hypoxic BJAB and BJAB-KSHV cells compared to that in normoxic BJAB cells. (J) Fold change expression of genes involved in histidine metabolism in normoxic BJAB-KSHV or hypoxic BJAB and BJAB-KSHV cells compared to that in normoxic BJAB cells. (K) Fold change expression of genes involved in proline metabolism in normoxic BJAB-KSHV or hypoxic BJAB and BJAB-KSHV cells compared to that in normoxic BJAB cells. (L) Fold change expression of genes involved in serine, glycine, and threonine metabolism in normoxic BJAB-KSHV or hypoxic BJAB and BJAB-KSHV cells compared to that in normoxic BJAB cells. (M) Fold change expression of genes involved in glutamine and glutamate metabolism in normoxic BJAB-KSHV or hypoxic BJAB and BJAB-KSHV cells compared to that in normoxic BJAB cells.

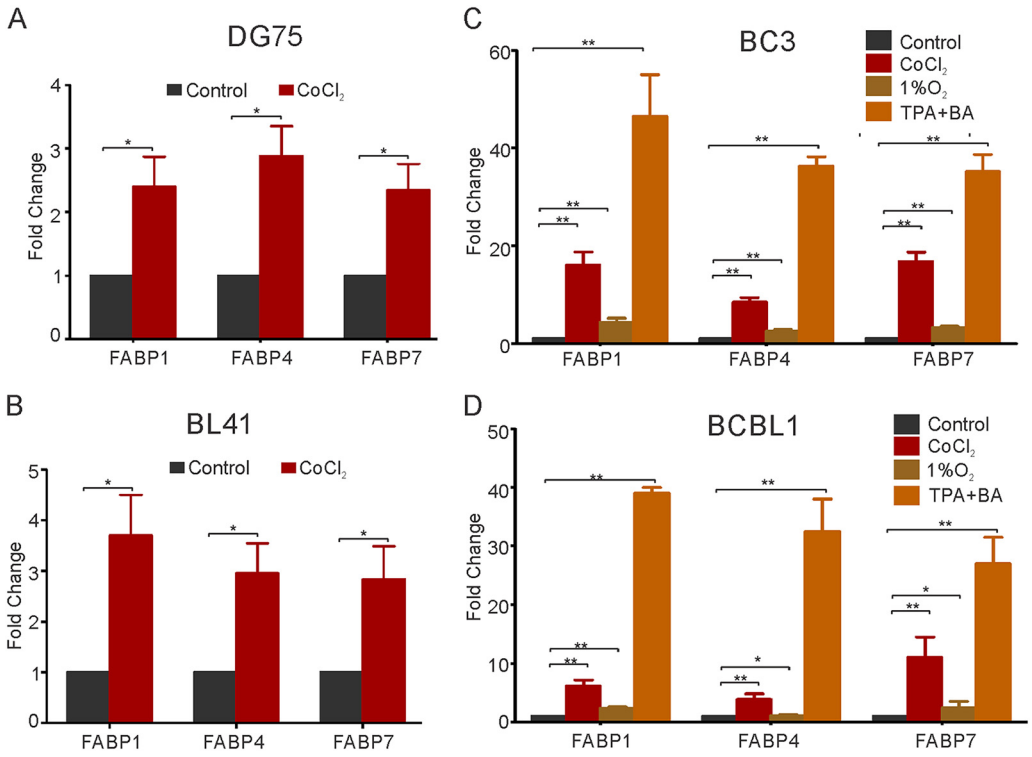

FIG 3 Comparative analysis of differential gene expression of FABPs in KSHV-negative (DG75 and BL41) and KSHV-positive (BC3 and BCBL1) cells. (A) Fold change expression of FABP1, FABP4, and FABP7 in $CoCl_2$-induced hypoxic DG75 cells compared to that in normoxic cells. Cells were grown under normoxic or $CoCl_2$-induced hypoxic conditions for 48 h. Fold change expression was measured using real-time PCR. GAPDH was used as an endogenous control. (B) Fold change expression of FABP1, FABP4, and FABP7 in $CoCl_2$-induced hypoxic BL41 cells compared to that in normoxic BL41 cells. Cells were grown under normoxic or $CoCl_2$-induced hypoxic conditions for 48 h. Fold change expression was measured using real-time PCR. GAPDH was used as an endogenous control. (C) Fold change expression of FABP1, FABP4, and FABP7 in $CoCl_2$/1% O_2/TPA and butyric acid-treated KSHV-positive BC3 cells compared to that in normoxic cells. Cells were grown under normoxic or mentioned treatment conditions for 48 h. Fold change expression was measured using real-time PCR. GAPDH was used as an endogenous control. (D) Fold change expression of FABP1, FABP4, and FABP7 in $CoCl_2$/1% O_2/TPA and butyric acid-treated KSHV-positive BCBL1 cells compared to that in normoxic cells. Cells were grown under normoxic or $CoCl_2$-induced hypoxic conditions for 48 h. Fold change expression of target genes were calculated using GAPDH as an endogenous control.

shown to be upregulated in BJAB cells grown in hypoxia. Interestingly, only KMO and TPH2 (tryptophan metabolic pathway), ALDH3B1, and MAOA (histidine metabolic pathway) were upregulated in BJAB-KSHV cells grown in hypoxia. Moreover, we observed some genes that were exclusively upregulated in only BJAB-KSHV cells grown in normoxia, included CYP1B1, DDC, KMO, OGDHL, TPH2 and WARS (tryptophan metabolic pathway), ALDH3B1, CNDP1, FTCD, and WBSCR22 (histidine metabolic pathway) (Fig. 2B and J).

Synergistic regulation of fatty acid binding protein gene family in naturally infected KSHV-positive cells in hypoxia. Based on the results of differential gene expression of fatty acid and amino acid metabolic pathway genes in BJAB-KSHV or BJAB cells grown in normoxia and hypoxia, we investigated the fatty acid binding protein (FABP) family of genes in detail. The FABPs members FABP1, FABP4, and FABP7 were shown to be upregulated in hypoxia by KSHV and were synergistically increased with both KSHV and hypoxia. To corroborate the results of differential gene expression in a naturally infected KSHV cell background, we investigated the gene expression profiles of FABP1, FABP4, and FABP7 in two additional KSHV-negative cell lines (DG75 and BL41) and compared them with those of two naturally infected KSHV-positive cell lines (BC3 and BCBL1) (Fig. 3A to D). Induction of hypoxia was done by treating these cells with $CoCl_2$ and validating by analyzing the upregulation of the downstream HIF1α transcriptional target P4HA1 in these cells (data not shown). The results of differential

gene expression for FABP1, FABP4, and FABP7 in KSHV-negative DG75 and BL41 cells showed that these transcripts were upregulated due to hypoxia. In DG75 cells, an upregulation of 2.5-, 2.8-, and 2.4-fold for FABP1, FABP4, and FABP7, respectively, was observed (Fig. 3A). Similarly, in BL41 cells, FABP1, FABP4, and FABP7 were upregulated by 3.8-, 2.9-, and 2.8-fold, respectively (Fig. 3B). Next, we investigated the effect of hypoxia on the expression of FABP1, FABP4, and FABP7 in KSHV-positive BC3 and BCBL1 cell lines. As expected, hypoxia induced expression of all three FABPs, but the magnitude of upregulation was dramatically higher than that compared to KSHV-negative DG75 and BL41 cells. In brief, the fold change for FABP1, FABP4, and FABP7 in BC3 cells growing under hypoxic conditions were approximately 18-, 10-, and 15-fold, respectively (Fig. 3C). Similarly, the fold change expressions of FABP1, FABP4, and FABP7 in BCBL1 cells growing under hypoxic conditions were more than double those seen in BL41 cells (Fig. 3D). These results confirm that hypoxia can induce expression of the FABP family transcripts and that KSHV infection can further amplify the effect.

As hypoxia is known to promote KSHV reactivation in infected cells, we hypothesized that upregulation of the fatty acid binding proteins may be a prerequisite for KSHV reactivation. To validate our hypothesis, we treated KSHV-positive cells (BC3 and BCBL1) with TPA/BA to reactivate the cells and investigated the differential gene expression of FABP1, FABP4, and FABP7 in treated cells compared to that in control cells. KSHV reactivation in both BC3 and BCBL1 cells was monitored by detection of the replication and transcriptional activator (RTA) by immune-fluorescence imaging (data not shown). Analysis of differential gene expression of FABPs showed that treatment of KSHV-positive cells with TPA/BA had a dramatic effect on the activation of expression of these FABP transcripts. In BC3 cells, expression of FABP1, FABP4, and FABP7 was increased by 51-, 36-, and 35-fold, respectively, upon TPA/BA treatment and reactivation (Fig. 3C). Similarly, in BCBL1 cells, expression of FABP1, FABP4, and FABP7 was 40-, 32-, and 28-fold, respectively, upon TPA/BA treatment and reactivation (Fig. 3D). To further, support our results, which showed FABP upregulation due to KSHV in physiological conditions, BC3 and BCBL1 cells were grown in low oxygen hypoxia conditions with 1% oxygen. Interestingly, hypoxia also showed upregulation of FABPs compared to those in normoxic cells, although the fold change difference was lower compared to that in the $CoCl_2$ or TPA/BA treatment (Fig. 3C and D). This may be due to the inhibitory effect of low oxygen on mitochondrial energy generation or inhibition of transcription under conditions of low oxygen. These results clearly demonstrated that hypoxia as well as KSHV can modulate the expression of FABP transcripts alone or in combination resulting in a synergistic effect and suggest a direct role in KSHV reactivation.

KSHV-encoded vGPCR and LANA can regulate expression of FABPs in hypoxia. Based on the results showing that the presence of KSHV has a synergistic role on upregulation of FABPs, we hypothesized that one or more KSHV-encoded factor(s) must be involved in this transcriptional regulation. Since KSHV-encoded LANA, RTA, vCyclin, and vGPCR are well-known antigens being upregulated in hypoxic conditions, we hypothesized that one or more of these antigens are responsible for synergistic transactivation of FABPs. To test our hypothesis, we expressed these antigens into HEK293T cells and investigated the transactivation potential of these antigens on FABP gene expression. Heterogeneous expression of these viral encoded genes was confirmed by Western blotting against the epitope tag (myc) fused to the genes (Fig. 4A to D). Analysis of the differential expression for FABP genes suggested a substantial role of vGPCR and LANA on the transcriptional activation of FABP genes. We observed that vGPCR expression was highly effective in inducing expression of FABPs, where expression of FABP1, FABP4, and FABP7 was found to be upregulated by 46-, 8-, and 19-fold, respectively. Similarly, LANA expression also showed a similar upward trend of induction of FABP gene expression, with an upregulation of 9-, 5-, and 7.5-fold for FABP1, FABP4, and FABP7, respectively. RTA expression also resulted in an enhanced effect on expression of FABP transcripts, although the effect was not as evident as that shown

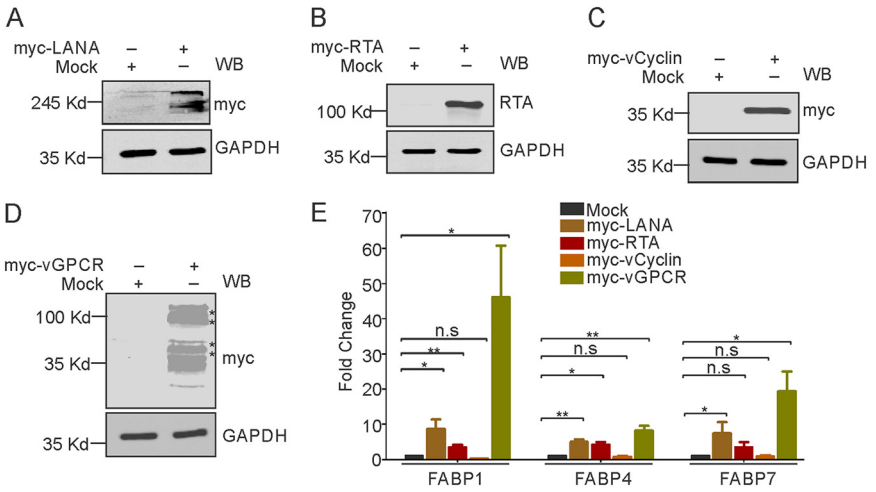

FIG 4 KSHV-encoded LANA and vGPCR positively upregulates expression of FABP1, FABP4, and FABP7. (A to D) Expression of KSHV-encoded LANA, RTA, vCyclin, and vGPCR in HEK293T cells. Mock or myc-tagged constructs of LANA, RTA, vCyclin, and vGPCR were transfected in HEK293T cells. At 48 h posttransfection, cells were lysed and equal amounts of whole-cell lysate were used to detect expression by Western blot analysis using anti-Myc antibodies. Asterisks in vGPCR Western blot represent aggregated proteins running upward, generally observed for several hydrophobic membrane proteins. (E) Real-time PCR analysis for FABP1, FABP4, and FABP7 in LANA, RTA, vCyclin, or vGPCR expressing HEK293T cells compared to mock-transfected cells. At 48 h posttransfection, RNA was isolated by standard phenol chloroform extraction. Two micrograms of RNA was used to synthesize cDNA. Fold change expression of FABP1, FABP4, and FABP7 in LANA-, RTA-, vCyclin-, or vGPCR-transfected cells was compared to that in mock-transfected cells by real-time PCR using GAPDH as the endogenous control.

by vGPCR or LANA expression. Interestingly, we observed a small suppressive effect on FABP genes when vCyclin was expressed.

Overall, expression of KSHV-encoded genes, as well as expression analysis, strongly suggested that the upregulation of FABP gene expression was mediated via the HIF1α-dependent pathways. Further corroborative studies were done by investigating the results at the protein level. We performed Western blot analysis against FABP1, FABP4, and FABP7 from whole-cell lysate of BJAB and BJAB-KSHV cells grown in normoxic or $CoCl_2$-induced hypoxic conditions. Our results clearly showed that KSHV and hypoxia can synergistically upregulate expression of these FABPs at the transcript as well as protein levels (Fig. 5A). We also validated the results of LANA- and vGPCR-mediated induction of FABP1, FABP4, and FABP7 transcripts at the protein level. For this, we performed a Western blot analysis from whole-cell lysates of HEK293T cell expression for either LANA or vGPCR genes compared to mock-expressing cells. The vCyclin and RTA gene constructs were also used in a transfection experiment to completely rule out their role in FABP expression. Western blot analyses for FABP1, FABP4, and FABP7 clearly showed that expression of both LANA and vGPCR were able to induce expression of FABP1, FABP4, and FABP7 at the protein level compared to that of mock-transfected cells (Fig. 5B). As LANA and vGPCR are known for their stabilizing or transactivating effect on HIF1α, we also included HIF1α Western blotting to correlate LANA- and vGPCR-dependent transactivation of these FABPs.

Knockdown of FABP gene transcripts negatively impacted KSHV reactivation in hypoxia. We further investigated whether knocking down FABPs in KSHV-positive cells can have a compromising effect on hypoxia-mediated reactivation. We designed short hairpin RNA (shRNA) oligonucleotides targeting FABP1, FABP4, or FABP7 and cloned them into a lentiviral-based plasmid vector. Although we did not observe a significant knockdown by the ShFABP4 construct, we included this construct in the study as a negative control. Lentiviruses encoding shRNA for FABP1, FABP4, or FABP7 were used to transduce KSHV-positive BC3 cells. The transduction by ShFABP1, ShFABP4, or ShFABP7 encoding lentiviruses was confirmed by visualizing green fluorescence

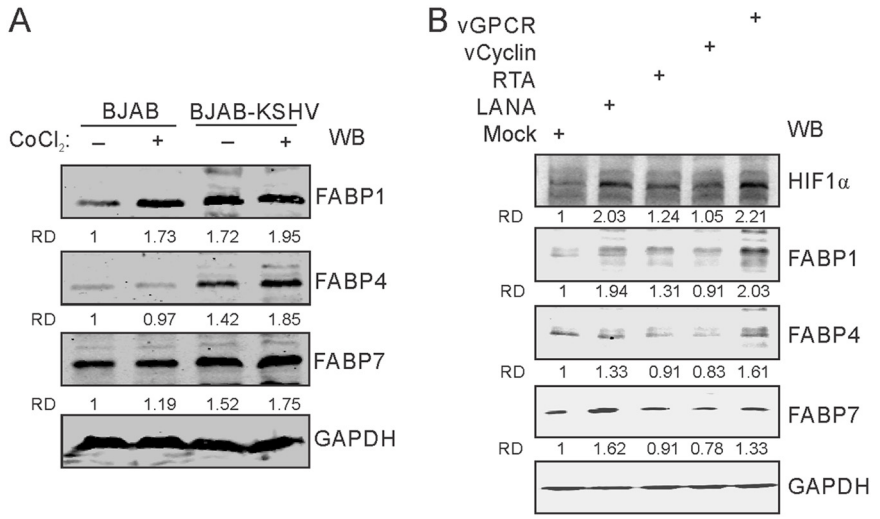

FIG 5 Confirmation of FABP1, FABP4, and FABP7 upregulation by KSHV in hypoxic conditions at the protein level. (A) BJAB and BJAB-KSHV cells were grown under normoxic or $CoCl_2$-induced hypoxic conditions for 48 h. Cells were lysed, and equal amounts of whole-cell lysate were electrophoresed on polyacrylamide gel followed by transfer to nitrocellulose membrane. Expression levels of FABP1, FABP4, or FABP7 were monitored by Western blot analysis using specific antibodies against respective proteins. GAPDH served as loading control. (B) Confirmation of FABP1, FABP4, and FABP7 upregulation by KSHV-encoded LANA and vGPCR at protein levels. HEK293T cells were transfected with mock, LANA, vGPCR, vCyclin, or RTA constructs. At 48 h posttransfection, cells were lysed, and equal amounts of whole-cell lysate were electrophoresed on polyacrylamide gel followed by transfer to nitrocellulose membrane. Expression levels of FABP1, FABP4, or FABP7 were monitored by Western blot analysis using specific antibodies against respective proteins. GAPDH served as a loading control.

protein (Fig. 6A). Stable cell lines with transduced ShFABP1, ShFABP4, or ShFABP7 encoding lentiviruses were generated by selecting the cells in puromycin containing medium for 3 weeks. Knockdown of FABP1, ShFABP4, and FABP7 transcripts were analyzed by real-time PCR using gene-specific primers (Fig. 6B, C, and D). BC3-ShControl, BC3-ShFABP1, BC3-ShFABP4, and BC3-ShFABP7 cells were challenged for induction of reactivation by hypoxia for 72 h by treating with $CoCl_2$. ShControl and ShFABP1 expressing cells treated with $CoCl_2$ was used as a representative sample to confirm induction of the lytic cycle by monitoring expression of KSHV-encoded RTA (data not shown). BC3-ShControl cells treated with TPA were also used as a positive control. The extracellular medium was collected and centrifuged to remove cellular debris. The supernatant was further passed through a 0.45-μm membrane filter followed by collection of the KSHV virions using standard protocol of ultracentrifugation described in Materials and Methods (30). The concentrated KSHV virions were used to isolate DNA, and the copy number was calculated. The results showed that the BC3-ShFABP1 cells are highly compromised in terms of generating extracellular KSHV virions when experiencing hypoxic conditions compared to BC3-ShControl cells (Fig. 6D). BC3-ShFABP7 cells were also compromised in their ability to generate extracellular KSHV virions under hypoxic conditions compared to BC3-ShControl cells, although the effect was not as severe as BC3-ShFABP1 cells (Fig. 6D). Further, BC3-ShFABP4-negative control cells behaved like ShControl cells, confirming the role of FABPs in hypoxic reactivation of KSHV. These results strongly suggested that induction of FABP gene expression by KSHV-encoded antigens in hypoxia is critical for hypoxia-mediated reactivation of KSHV.

DISCUSSION

Cellular metabolic reprogramming is closely associated with infection of various pathogens, including viruses (42–44). In general, metabolic reprograming is essential for efficient persistence of pathogens within host cells, reactivation, as well as

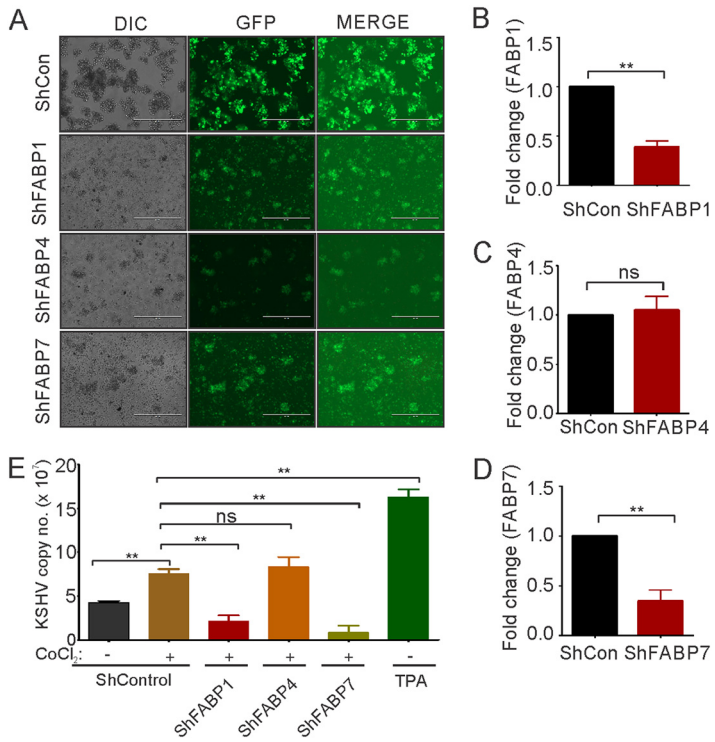

FIG 6 FABP knockdown cells showed compromised potential for KSHV reactivation under hypoxic conditions. (A) Generation of ShFABP1, ShFABP4, and ShFABP7 cell lines in KSHV-positive BC3 cells. Lentiviral particles generated in HEK293T cells and encoding shRNA for FABP1, FABP4, or FABP7 were used for infecting BC3 cells. The cells were selected in puromycin-containing medium for 3 weeks. GFP expressing green cells represent stably infected cells expressing shRNA for FABP1, FABP4, or FABP7. (B) Real-time PCR was used for analyzing knockdown of FABP1 in ShFABP1 stable cells compared to that in ShControl cells using GAPDH as an endogenous control. (C) Real-time PCR was used for analyzing knockdown of FABP4 in ShFABP4 stable cells compared to that in ShControl cells using GAPDH as an endogenous control. (D) Real-time PCR was used for analyzing knockdown of FABP7 in ShFABP7 stable cells compared to that in ShControl cells using GAPDH as an endogenous control. (E) Copy number calculation from extracellular medium of ShFABP1, ShFABP4, and ShFABP7 cells compared to that from ShControl cells induced for $CoCl_2$-mediated hypoxic reactivation. TPA treatment was taken as a positive control. Cells were grown under normal medium, $CoCl_2$-, or TPA-containing medium for 72 h. Extracellular medium was collected followed by centrifugation at 3,000 rpm to remove any particulate debris. The medium was then filtered through a 0.45-μm filter and subjected for ultracentrifugation to pellet down produced viral particles. DNA isolated from pelleted viral particle was used for copy number calculation using standard curve method.

pathogenesis (45, 46). KSHV, an oncogenic herpesvirus, has also been associated with metabolic reprogramming of infected cells (47, 48). KSHV, like many other herpesviruses, is known to exhibit two distinct patterns during its life cycle, a latent and a lytic phase (49, 50). Once inside an infected cell, the KSHV genome undergoes a series of epigenetic modifications (mainly histone modifications) before it tethers itself to the cellular genome as episomal DNA. These epigenetic modifications allow expression of only a limited number of genes encoded by KSHV, which are essential for KSHV genome persistence. In general, during the latent phase of the KSHV life cycle, LANA, vCyclin, and vFLIP (expressed from the same promoter) are major antigens expressed in infected cells. Notably, analysis from certain KSHV-positive biopsy samples also provide evidence for the presence of vGPCR, vIRFs, and kaposin (10). While only limited conditions are known to allow a switch from latency to lytic cycle, reversal of epigenetic reprogramming of KSHV genome is essential for this to happen. Hypoxia, metabolic stress, imbalances in reactive oxygen species, or the presence of chemicals that can cause epigenetic modification of genomes are well-established factors, which induce reactivation of KSHV from latency. The KSHV-encoded replication and

transcriptional activator (RTA) is critical for driving the lytic cycle of KSHV and mediates transcriptional activation of all KSHV-encoded genes whose products are required for assembly and packaging of new infectious KSHV virions. Both the latent and lytic cycle of KSHV is known to reprogram cellular metabolism through many different pathways. Induction of the glycolysis, glutaminolysis, and fatty acid synthetic pathways by KSHV is essential for survival of latently infected cells (51). Nevertheless, mitochondrial functioning is also essential for the survival of KSHV-infected cells, where KSHV-encoded antigens interact and modulate the mitochondrial system (52). In another approach investigating cellular transformation of mouse mesenchymal stem cells by KSHV, it was shown that these cells do not require glucose for growth or production of anchorage-independent colonies (53). However, a look at amino acid metabolism showed that the presence of glutamine in culture medium was essential and that KSHV-positive cells are glutamine addicted (54). Additionally, inhibition of these pathways can negatively impact productive replication of KSHV. Specifically, inhibition of the glycolysis and glutaminolysis was observed to block viral replication but is essential for early gene expression and translation during productive replication of KSHV (51). Additionally, dysregulation in fatty acid synthesis and glycolysis has been reported in viral infection-associated lymphoma (55).

In the present study, we aimed to investigate the transcriptional signature of genes involved in fatty acid and amino acid biosynthetic pathways in KSHV-positive cells and in KSHV-negative and KSHV-positive BJAB cells grown under normoxic or hypoxic conditions. The chemical induced hypoxia allowed a higher level of induced HIF1α, which is a general characteristic of KSHV as well as other oncogenic virus-infected cells. It is also known that HIF1α in conjugation with KSHV-encoded LANA can transactivate KSHV-encoded immediate early RTA (19). Hypoxia-induced RTA transactivation is reported for KSHV reactivation in response to hypoxia (19). Using this strategy, we studied the conversing transcriptional signature of KSHV-positive cells with respect to KSHV-negative cells of the same isogenic background grown in hypoxic conditions. We also investigated the transcriptional signature of KSHV-positive cells grown in hypoxia compared with normoxic conditions for BJAB or BJAB-KSHV cells. We investigated the fold change in expression of genes involved in fatty acid metabolism (acetyl-CoA, fatty acid transport, carnitine, triacylglycerol, ketogenesis, and ketone body) and amino acid metabolism (arginine, glutamine and glutamate, leucine, proline, tryptophan, methionine, isoleucine, histidine, alanine, phenylalanine, serine, glycine, threonine, tyrosine, and valine). We observed a distinct pattern of gene expression in both BJAB and BJAB-KSHV cells grown in hypoxic conditions. In most cases, treatment of these cells with $COCl_2$, which induced hypoxia, resulted in downregulation of expression, except for some genes, including FABP1, FABP, and FABP7 (fatty acid metabolism); CPT1A, CRAT, and CROT (carnitine metabolism); ACADL, ACADVL, ACSBG1, ACSL3, ACOT6, ACOT12, PRKAA2, PRKAB1, PRKACA (acetyl-CoA metabolism); AOC1, AMD1, and SAT1 (arginine metabolism); AOX1 (leucine metabolism); KMO1 and TPH2 (tryptophan metabolism); MAT1A (methionine metabolism); MAOA (histidine metabolism); and HGD (tyrosine metabolism). Among these genes, we further investigated in greater detail the FABPs FABP1, FABP4, and FABP7 based on their roles in fatty acid transportation, which may represent a crucial event during synthesis of viral membrane during hypoxic reactivation. First, we corroborated the result of this initial screening in two naturally infected KSHV-positive B-cells, BC3 and BCBL1. Here, we included an alternate approach to inducing hypoxia by growing these in 1% O_2 condition. Also, to corroborate the role of FABPs in KSHV reactivation, we used TPA-treated cells. Interestingly, we observed an upregulation of the FABP (FABP1, FABP4, and FABP7) genes under all treatment conditions ($CoCl_2$, 1% O_2, and TPA). To investigate whether the upregulated expression of FABPs is a typical characteristic of hypoxia irrespective of KSHV background, we investigated the expression of these proteins in two KSHV-negative DG75 and BL41 cell lines. We observed a small increase in expression in the range of 2- to 4-fold in these cell lines compared to a 10- to 20-fold upregulated expression in the KSHV-positive BC3 or

BCBL1 cells. This suggested that, in addition to hypoxia, other antigens encoded by KSHV synergistically worked to enhance upregulation of the FABP genes. We transfected HEK293T cells with KSHV-encoded genes, which are expressed during latency or hypoxic conditions, including LANA, RTA, vCyclin, and vGPCR (10, 31). Although, a small upregulation of the investigated FABPs was observed in LANA- and RTA-expressing cells, a dramatic increase in their expression between 20- and 40-fold was observed in vGPCR-expressing cells compared to that of control cells. These results clearly indicated that stabilization of HIF1α by KSHV-encoded LANA, possibly through degradation of the VHL protein, or its positive regulation by KSHV-encoded vGPCR through the MAPK/P38 pathway, was a critical component driving hypoxia-induced expression of the FABP genes.

We finally investigated whether upregulation of FABP genes has any direct impact on KSHV reactivation in hypoxic conditions. Stable knockdown of two representative FABPs (FABP1 and FABP7) was generated in KSHV-positive BC3 cells through the short hairpin RNA interference method. ShControl or ShFABP cells were challenged for their ability to reactivate through hypoxia induction based on their ability to make copies of KSHV. Analysis of the copy number of KSHV from ShControl and ShFABP cells generated in response to hypoxia clearly indicated that upregulated FABPs in hypoxia was an essential criteria for viral reactivation.

The expression of different fatty acid binding proteins is known to be tissue specific, and their expression in B-cells at transcript or protein levels are not well studied. Our current study explored the role of FABPs in the biology of KSHV-infected cells. Overall, these studies now provide new potential targets for innovative therapeutic approaches using inhibitors of FABPs to potentially control KSHV-associated malignancies.

MATERIALS AND METHODS

Cell culture and treatments. KSHV-negative BJAB cells were provided by Elliot Kieff (Harvard Medical School, Boston, MA). BJAB-KSHV was a generous gift from Michael Luganoff (University of Washington, Seattle, WA). BC3-ShControl cells were generated and described earlier (31, 56). KSHV-positive cells BC3 and BCBL1 and KSHV-negative cells DG75 and BL41 were described earlier (30). All B-cell lines were grown at 37°C/5% CO_2 in RPMI medium supplemented with 7% bovine growth serum (BGS), 100 units/ml penicillin, and 0.1 mg/ml streptomycin. BJAB-KSHV, BC3-ShControl, and BC3-ShFABP cells were maintained in additional selection of 2 μg/ml puromycin. HEK293T cells were maintained in Dulbecco modified Eagle medium (DMEM) supplemented with 7% bovine growth serum (BGS), 100 units/ml penicillin, and 0.1 mg/ml streptomycin at 37°C/5% CO_2. For chemical induction of hypoxia, cells were treated with 100 μM $CoCl_2$ for 48 h in complete medium and incubated at 37°C in a CO_2 incubator. Low oxygen hypoxic treatment was performed by growing the cells in hypoxic chamber with 1% oxygen setting.

Plasmids, transfection. The pA3F-LANA, pCEFL-vGPCR, pEF1-myc-RTA, and pLVX-AC-GFP-vCyclin plasmids (described earlier [30]) were used to PCR amplify LANA, vGPCR, RTA, and vCyclin. The myc-tagged constructs of LANA, vGPCR, RTA, and vCyclin were generated by restriction digestion and ligation of PCR products into the pA3M plasmid vector (30). Transfection of HEK293T cells was performed in a 6-well plate at 60 to 70% confluence using jetPrime reagent (Polyplus-transfection, New York, NY) according to manufacturer protocol.

Viral DNA isolation and copy number calculation. The supernatant from KSHV-positive BC3 cells (ShControl, ShABP1, ShFABP4, and ShFABP7) grown under normoxic or hypoxic conditions was centrifuged at 3,000 rpm to remove any possible cell debris. The medium was then filtered through a 0.45-μm membrane. The filtered medium was loaded for ultracentrifugation at speeds of 23,500 rpm for 2 h at 4°C. Supernatant from the ultracentrifugation tube was aspirated, leaving approximately 0.5 ml to avoid disturbing the viral pellet. The ultracentrifugation steps were repeated as needed until the total volume of supernatant was centrifuged. Finally, the viral pellets were resuspended by pipetting up and down 10 times and left at 4°C overnight for complete resuspension under aseptic conditions. To isolate viral DNA, the viral suspension was mixed with equal volumes of 2$\times$ lysis buffer (20 mM Tris, pH 8.0; 2 mM EDTA; and 300 mM NaCl). The virus-lysis buffer mix was added with SDS and proteinase K at a final concentration of 1% (wt/vol) and 1 mg/ml, respectively. The mixture was incubated at 55°C for 1 h, and the genomic DNA was isolated using standard phenol-chloroform extraction. KSHV copy number was calculated by the standard curve method using real-time PCR. Briefly, the known number of KSHV copies was based on the genomic region (coordinates, 85820 to 100784) cloned in a cosmid vector, which was used to generate a standard curve (30 to 300,000 copies in multiples of 10-fold). Genomic DNA isolated from purified KSHV virions from equal volumes of filtered supernatants was used to calculate the comparative number of KSHV virions generated in response to hypoxia.

Lentivirus preparation and infection. Generation of BC3-ShControl cells was described earlier (56). To generate ShFABP1, ShFABP4, and ShFABP7 constructs, oligonucleotides encoding respective shRNA

were cloned into MluI/XhoI restriction sites of pGZIP plasmid vector (56). The positive constructs for ShFABP1, ShFABP4, and ShFABP7 were screened by restriction digestion followed by confirmation through DNA sequencing. To generate lentiviral particles, shRNA constructs along with packaging and helper plasmids were transfected in HEK293T cells using the calcium phosphate method. At 24 h post-transfection, the medium was replaced with fresh medium containing sodium butyrate and HEPES, which was collected after 12 h and replaced again with fresh medium containing sodium butyrate and HEPES. The collected media were kept at 4°C, and the collection and replacement of media were repeated 4 times. The collected pooled media were centrifuged at 3,000 rpm to remove cell debris, and the clear fractions were filtered through 0.45-μm membrane filters. The filtered media were subjected to ultracentrifugation at 23,500 rpm for 2 h. The supernatants were aspirated, and the lentivirus pellets were each resuspended in 1 ml of serum-free medium. To perform infection with concentrated lentivirus, 2 million cells were harvested and resuspended in 1 ml of concentrated lentivirus particles. Polybrene at a final concentration of 20 μg/ml was then added, and the infection mixtures were mixed by pipetting up and down several times. The infections were then incubated at 37°C with 5% CO_2 for 4 h. After incubation, the infection mixtures were centrifuged, and the supernatant aspirated. The cell pellets were resuspended into 2 ml of serum containing fresh medium and transferred to individual wells of 6-well plates. At 48 h postincubation, cells were grown in medium containing 2 μg/ml puromycin. The selection was performed for 3 weeks until cells showed positive green fluorescence signals at 100% indicating a clonal population. After selection, cells were maintained in 1 μg/ml puromycin.

RNA isolation, cDNA preparation, and real-time PCR. Total RNA from cells grown in culture were isolated by standard phenol chloroform extraction method using TRIzol (Ambion, Grand Island, NY). Briefly, cell pellets were directly lysed in 0.5 to 1 ml TRIzol and kept at room temperature to disrupt cellular organelles including the nucleus. The lysates were mixed with 0.1 to 0.2 ml chloroform followed by mixing. The mixtures were kept at room temperature for 5 min followed by centrifugation at 13,000 rpm for 10 min. The aqueous phases were collected into fresh tubes, and the RNA was precipitated using 0.25 to 0.5 ml of isopropanol. The precipitated RNA was pelleted by centrifugation at 13,000 rpm for 10 min. RNA pellets were washed with 70% ethanol and semidried at room temperature. The RNA pellets were resuspended in RNase-free water by pipetting up and down. Finally, the resuspended pellets were kept at 55°C for 5 min and the RNA concentrations estimated using nanodrop spectrophotometry. The cDNAs were synthesized from 2 μg of total cellular RNA by random hexamer primers using SuperScript cDNA synthesis kit (Applied Biosystems, Inc., Foster City, CA). Synthesized cDNA was diluted 10-fold and 1 μl of diluted cDNA used for real-time PCR using SYBR green reagent (Applied Biosystems, Inc., Carlsbad, CA) on a StepOnePlus or QuantStudio 5 system (Applied Biosystems, Inc., Carlsbad, CA). The fold change differences calculated by the $\Delta\Delta CT$ method using default parameter settings. Details for the threshold cycle (C_T) value for all genes examined are provided in Data Set S1 in the supplemental material.

Western blotting and microscopy. Whole-cell lysates were prepared by lysing the cells in radioimmunoprecipitation assay (RIPA) buffer containing protease inhibitors (aprotinin, leupeptin, pepstatin, and 1 mM phenylmethylsulfonyl fluoride [PMSF]). Equal amounts of proteins were separated on sodium dodecyl sulfate-polyacrylamide gel followed by transfer onto nitrocellulose membrane. Skimmed milk (5% in Tris-buffered saline with Tween 20 [TBST]) was used to block membranes for 1 h at room temperature with mild shaking. Primary antibodies against glyceraldehyde-3-phosphate dehydrogenase (GAPDH), FABP1, FABP4, and FABP7 (Santa Cruz Inc., Dallas, TX); myc (purified ascites from hybridomas; a kind gift from Richard M. Longnecker, University of Northwestern University); and RTA (purified ascites from hybridomas; a kind gift from Ke Lan, Institut Pasteur of Shanghai) were incubated with membranes overnight at 4°C. Membranes were washed 3 times with TBST buffer for 5 min each followed by incubation with infrared (IR)-conjugated secondary antibodies. The blots were captured on Odyssey Scanner (LiCor Inc., Lincoln, Nebraska). For confocal microscopy, cells were seeded and semidried on 8-well slides followed by fixation in 4% paraformaldehyde. The slides were washed 3 times (5 min each) with phosphate-buffered saline followed by a combination of permeabilization and blocking (3% bovine serum albumin [BSA] in phosphate-buffered saline [PBS] with 0.1% Triton X-100). Primary antibody incubations were done at 4°C overnight. Slides were washed 3 times with PBS followed by incubation with Alexa Fluor-conjugated secondary antibody at room temperature for 1 h. DAPI (4′,6-diamidino-2-phenylindole) staining was performed for 20 min followed by washing and mounting.

Statistical analysis. All the statistical analyses performed in this study were made using freely available GraphPad Prism software (GraphPad, San Diego, CA). The mean values with standard error of mean were presented in this study when appropriate. Statistical significance based on fold change in expression of different sets of experiment was calculated by performing a 2-tailed Student's *t* test. The *P* value of <0.05 was considered statistically significant. NS, not significant; *, *P* value < 0.05; **, *P* value < 0.01.

SUPPLEMENTAL MATERIAL

Supplemental material is available online only.

SUPPLEMENTAL FILE 1, PDF file, 0.2 MB.

SUPPLEMENTAL FILE 2, XLSX file, 0.1 MB.

ACKNOWLEDGMENTS

We are grateful to Enrique A. Mesri (Miller school of Medicine, University of Miami) for kindly providing the pCEFL-vGPCR construct.

This work was supported by the National Cancer Institute at the National Institutes of Health under award numbers P30-CA016520, P01-CA174439, R01-CA171979, and R01-CA244074 (to E.S.R.). E.S.R. was a scholar of the Leukemia and Lymphoma Society of America. The funders had no role in study design, data collection and analysis, the decision to publish, or preparation of the manuscript.

We declare that no financial or nonfinancial competing interest exists.

REFERENCES

1. Young LS, Yap LF, Murray PG. 2016. Epstein-Barr virus: more than 50 years old and still providing surprises. Nat Rev Cancer 16:789–802. https://doi.org/10.1038/nrc.2016.92.
2. Arias C, Weisburd B, Stern-Ginossar N, Mercier A, Madrid AS, Bellare P, Holdorf M, Weissman JS, Ganem D. 2014. KSHV 2.0: a comprehensive annotation of the Kaposi's sarcoma-associated herpesvirus genome using next-generation sequencing reveals novel genomic and functional features. PLoS Pathog 10:e1003847. https://doi.org/10.1371/journal.ppat.1003847.
3. Parravicini C, Chandran B, Corbellino M, Berti E, Paulli M, Moore PS, Chang Y. 2000. Differential viral protein expression in Kaposi's sarcoma-associated herpesvirus-infected diseases: Kaposi's sarcoma, primary effusion lymphoma, and multicentric Castleman's disease. Am J Pathol 156:743–749. https://doi.org/10.1016/S0002-9440(10)64940-1.
4. Traylen CM, Patel HR, Fondaw W, Mahatme S, Williams JF, Walker LR, Dyson OF, Arce S, Akula SM. 2011. Virus reactivation: a panoramic view in human infections. Future Virol 6:451–463. https://doi.org/10.2217/fvl.11.21.
5. Giffin L, Damania B. 2014. KSHV: pathways to tumorigenesis and persistent infection. Adv Virus Res 88:111–159. https://doi.org/10.1016/B978-0-12-800098-4.00002-7.
6. Juillard F, Tan M, Li S, Kaye KM. 2016. Kaposi's sarcoma herpesvirus genome persistence. Front Microbiol 7:1149. https://doi.org/10.3389/fmicb.2016.01149.
7. Uppal T, Banerjee S, Sun Z, Verma SC, Robertson ES. 2014. KSHV LANA–the master regulator of KSHV latency. Viruses 6:4961–4998. https://doi.org/10.3390/v6124961.
8. Wei F, Gan J, Wang C, Zhu C, Cai Q. 2016. Cell cycle regulatory functions of the KSHV oncoprotein LANA. Front Microbiol 7:334. https://doi.org/10.3389/fmicb.2016.00334.
9. Fakhari FD, Dittmer DP. 2002. Charting latency transcripts in Kaposi's sarcoma-associated herpesvirus by whole-genome real-time quantitative PCR. J Virol 76:6213–6223. https://doi.org/10.1128/jvi.76.12.6213-6223.2002.
10. Damania B. 2004. Oncogenic gamma-herpesviruses: comparison of viral proteins involved in tumorigenesis. Nat Rev Microbiol 2:656–668. https://doi.org/10.1038/nrmicro958.
11. Damania B. 2004. Modulation of cell signaling pathways by Kaposi's sarcoma-associated herpesvirus (KSHV/HHV-8). Cell Biochem Biophys 40:305–322. https://doi.org/10.1385/CBB:40:3:305.
12. Watanabe T, Sugimoto A, Hosokawa K, Fujimuro M. 2018. Signal transduction pathways associated with KSHV-related tumors. Adv Exp Med Biol 1045:321–355. https://doi.org/10.1007/978-981-10-7230-7_15.
13. Bhatt AP, Damania B. 2013. AKTivation of PI3K/AKT/mTOR signaling pathway by KSHV. Front Immunol 3:401. https://doi.org/10.3389/fimmu.2012.00401.
14. Jarviluoma A, Ojala PM. 2006. Cell signaling pathways engaged by KSHV. Biochim Biophys Acta 1766:140–158. https://doi.org/10.1016/j.bbcan.2006.05.001.
15. Aneja KK, Yuan Y. 2017. Reactivation and lytic replication of Kaposi's sarcoma-associated herpesvirus: an update. Front Microbiol 8:613. https://doi.org/10.3389/fmicb.2017.00613.
16. Miller G, Heston L, Grogan E, Gradoville L, Rigsby M, Sun R, Shedd D, Kushnaryov VM, Grossberg S, Chang Y. 1997. Selective switch between latency and lytic replication of Kaposi's sarcoma herpesvirus and Epstein-Barr virus in dually infected body cavity lymphoma cells. J Virol 71:314–324. https://doi.org/10.1128/JVI.71.1.314-324.1997.
17. Hopcraft SE, Pattenden SG, James LI, Frye S, Dittmer DP, Damania B. 2018. Chromatin remodeling controls Kaposi's sarcoma-associated herpesvirus reactivation from latency. PLoS Pathog 14:e1007267. https://doi.org/10.1371/journal.ppat.1007267.
18. Granato M, Gilardini Montani M, Angiolillo C, D'Orazi G, Faggioni A, Cirone M. 2019. Cytotoxic drugs activate KSHV lytic cycle in latently infected PEL cells by inducing a moderate ROS increase controlled by HSF1, NRF2 and p62/SQSTM1. Viruses 11:8. https://doi.org/10.3390/v11010008.
19. Cai Q, Lan K, Verma SC, Si H, Lin D, Robertson ES. 2006. Kaposi's sarcoma-associated herpesvirus latent protein LANA interacts with HIF-1α to upregulate RTA expression during hypoxia: latency control under low oxygen conditions. J Virol 80:7965–7975. https://doi.org/10.1128/JVI.00689-06.
20. Cai QL, Knight JS, Verma SC, Zald P, Robertson ES. 2006. EC5S ubiquitin complex is recruited by KSHV latent antigen LANA for degradation of the VHL and p53 tumor suppressors. PLoS Pathog 2:e116. https://doi.org/10.1371/journal.ppat.0020116.
21. Tanimoto K, Makino Y, Pereira T, Poellinger L. 2000. Mechanism of regulation of the hypoxia-inducible factor-1α by the von Hippel-Lindau tumor suppressor protein. EMBO J 19:4298–4309. https://doi.org/10.1093/emboj/19.16.4298.
22. Gossage L, Eisen T, Maher ER. 2015. VHL, the story of a tumour suppressor gene. Nat Rev Cancer 15:55–64. https://doi.org/10.1038/nrc3844.
23. Veeranna RP, Haque M, Davis DA, Yang M, Yarchoan R. 2011. Kaposi's sarcoma-associated herpesvirus latency-associated nuclear antigen induction by hypoxia and hypoxia-inducible factors. J Virol 86:1097–1108. https://doi.org/10.1128/JVI.05167-11.
24. Matsumura S, Fujita Y, Gomez E, Tanese N, Wilson AC. 2005. Activation of the Kaposi's sarcoma-associated herpesvirus major latency locus by the lytic switch protein RTA (ORF50). J Virol 79:8493–8505. https://doi.org/10.1128/JVI.79.13.8493-8505.2005.
25. Hammond EM, Denko NC, Dorie MJ, Abraham RT, Giaccia AJ. 2002. Hypoxia links ATR and p53 through replication arrest. Mol Cell Biol 22:1834–1843. https://doi.org/10.1128/mcb.22.6.1834-1843.2002.
26. Ng N, Purshouse K, Foskolou IP, Olcina MM, Hammond EM. 2018. Challenges to DNA replication in hypoxic conditions. FEBS J 285:1563–1571. https://doi.org/10.1111/febs.14377.
27. Martin L, Rainey M, Santocanale C, Gardner LB. 2012. Hypoxic activation of ATR and the suppression of the initiation of DNA replication through cdc6 degradation. Oncogene 31:4076–4084. https://doi.org/10.1038/onc.2011.585.
28. Davis DA, Rinderknecht AS, Zoeteweij JP, Aoki Y, Read-Connole EL, Tosato G, Blauvelt A, Yarchoan R. 2001. Hypoxia induces lytic replication of Kaposi sarcoma-associated herpesvirus. Blood 97:3244–3250. https://doi.org/10.1182/blood.v97.10.3244.
29. Zhang L, Zhu C, Guo Y, Wei F, Lu J, Qin J, Banerjee S, Wang J, Shang H, Verma SC, Yuan Z, Robertson ES, Cai Q. 2014. Inhibition of KAP1 enhances hypoxia-induced Kaposi's sarcoma-associated herpesvirus reactivation through RBP-Jκ. J Virol 88:6873–6884. https://doi.org/10.1128/JVI.00283-14.
30. Singh RK, Lamplugh ZL, Lang F, Yuan Y, Lieberman P, You J, Robertson ES. 2019. KSHV-encoded LANA protects the cellular replication machinery from hypoxia induced degradation. PLoS Pathog 15:e1008025. https://doi.org/10.1371/journal.ppat.1008025.
31. Singh RK, Lang F, Pei Y, Jha HC, Robertson ES. 2018. Metabolic reprogramming of Kaposi's sarcoma associated herpes virus infected B-cells in hypoxia. PLoS Pathog 14:e1007062. https://doi.org/10.1371/journal.ppat.1007062.
32. Sodhi A, Montaner S, Patel V, Zohar M, Bais C, Mesri EA, Gutkind JS. 2000. The Kaposi's sarcoma-associated herpes virus G protein-coupled receptor up-regulates vascular endothelial growth factor expression and secretion through mitogen-activated protein kinase and p38 pathways acting on hypoxia-inducible factor 1alpha. Cancer Res 60:4873–4880.

33. Furuhashi M, Hotamisligil GS. 2008. Fatty acid-binding proteins: role in metabolic diseases and potential as drug targets. Nat Rev Drug Discov 7:489–503. https://doi.org/10.1038/nrd2589.
34. Smathers RL, Petersen DR. 2011. The human fatty acid-binding protein family: evolutionary divergences and functions. Hum Genomics 5:170–191. https://doi.org/10.1186/1479-7364-5-3-170.
35. Liu RZ, Mita R, Beaulieu M, Gao Z, Godbout R. 2010. Fatty acid binding proteins in brain development and disease. Int J Dev Biol 54:1229–1239. https://doi.org/10.1387/ijdb.092976rl.
36. Bottasso Arias NM, García M, Bondar C, Guzman L, Redondo A, Chopita N, Córsico B, Chirdo FG. 2015. Expression pattern of fatty acid binding proteins in celiac disease enteropathy. Mediators Inflamm 2015:738563. https://doi.org/10.1155/2015/738563.
37. Furuhashi M. 2019. Fatty acid-binding protein 4 in cardiovascular and metabolic diseases. J Atheroscler Thromb 26:216–232. https://doi.org/10.5551/jat.48710.
38. Chmurzynska A. 2006. The multigene family of fatty acid-binding proteins (FABPs): function, structure and polymorphism. J Appl Genet 47:39–48. https://doi.org/10.1007/BF03194597.
39. Storch J, Thumser AE. 2010. Tissue-specific functions in the fatty acid-binding protein family. J Biol Chem 285:32679–32683. https://doi.org/10.1074/jbc.R110.135210.
40. Das R, Hammamieh R, Neill R, Melhem M, Jett M. 2001. Expression pattern of fatty acid-binding proteins in human normal and cancer prostate cells and tissues. Clin Cancer Res 7:1706–1715.
41. Xu Y, Xie Y, Shao X, Ni Z, Mou S. 2015. L-FABP: a novel biomarker of kidney disease. Clin Chim Acta 445:85–90. https://doi.org/10.1016/j.cca.2015.03.017.
42. Escoll P, Buchrieser C. 2018. Metabolic reprogramming of host cells upon bacterial infection: why shift to a Warburg-like metabolism? FEBS J 285:2146–2160. https://doi.org/10.1111/febs.14446.
43. Passalacqua KD, Purdy JG, Wobus CE. 2019. The inert meets the living: the expanding view of metabolic alterations during viral pathogenesis. PLoS Pathog 15:e1007830. https://doi.org/10.1371/journal.ppat.1007830.
44. Kahn RA, Fu H, Roy CR. 2002. Cellular hijacking: a common strategy for microbial infection. Trends Biochem Sci 27:308–314. https://doi.org/10.1016/s0968-0004(02)02108-4.
45. Eisenreich W, Rudel T, Heesemann J, Goebel W. 2019. How viral and intracellular bacterial pathogens reprogram the metabolism of host cells to allow their intracellular replication. Front Cell Infect Microbiol 9:42. https://doi.org/10.3389/fcimb.2019.00042.
46. Sanchez EL, Lagunoff M. 2015. Viral activation of cellular metabolism. Virology 479–480:609–618. https://doi.org/10.1016/j.virol.2015.02.038.
47. Goncalves PH, Ziegelbauer J, Uldrick TS, Yarchoan R. 2017. Kaposi sarcoma herpesvirus-associated cancers and related diseases. Curr Opin HIV AIDS 12:47–56. https://doi.org/10.1097/COH.0000000000000330.
48. Molloy S. 2014. Viral infection: KSHV flicks the metabolic switch. Nat Rev Microbiol 12:723. https://doi.org/10.1038/nrmicro3377.
49. Ye F, Lei X, Gao SJ. 2011. Mechanisms of Kaposi's sarcoma-associated herpesvirus latency and reactivation. Adv Virol 2011:193860. https://doi.org/10.1155/2011/193860.
50. Jenner RG, Alba MM, Boshoff C, Kellam P. 2001. Kaposi's sarcoma-associated herpesvirus latent and lytic gene expression as revealed by DNA arrays. J Virol 75:891–902. https://doi.org/10.1128/JVI.75.2.891-902.2001.
51. Sanchez EL, Pulliam TH, Dimaio TA, Thalhofer AB, Delgado T, Lagunoff M. 2017. Glycolysis, glutaminolysis, and fatty acid synthesis are required for distinct stages of Kaposi's sarcoma-associated herpesvirus lytic replication. J Virol 91:e02237-16. https://doi.org/10.1128/JVI.02237-16.
52. Holmes DL, Vogt DT, Lagunoff M. 2020. A CRISPR-Cas9 screen identifies mitochondrial translation as an essential process in latent KSHV infection of human endothelial cells. Proc Natl Acad Sci U S A 117:28384–28392. https://doi.org/10.1073/pnas.2011645117.
53. Zhu Y, da Silva SR, Gao S-J. 2014. Metabolic reprogramming by KSHV in cellular transformation. Cancer Metab 2:P88. https://doi.org/10.1186/2049-3002-2-S1-P88.
54. Sanchez EL, Carroll PA, Thalhofer AB, Lagunoff M. 2015. Latent KSHV infected endothelial cells are glutamine addicted and require glutaminolysis for survival. PLoS Pathog 11:e1005052. https://doi.org/10.1371/journal.ppat.1005052.
55. Bhatt AP, Jacobs SR, Freemerman AJ, Makowski L, Rathmell JC, Dittmer DP, Damania B. 2012. Dysregulation of fatty acid synthesis and glycolysis in non-Hodgkin lymphoma. Proc Natl Acad Sci U S A 109:11818–11823. https://doi.org/10.1073/pnas.1205995109.
56. Jha HC, Sun Z, Upadhyay SK, El-Naccache DW, Singh RK, Sahu SK, Robertson ES. 2016. KSHV-mediated regulation of Par3 and SNAIL contributes to B-cell proliferation. PLoS Pathog 12:e1005801. https://doi.org/10.1371/journal.ppat.1005801.